AD-A034 676 GEORGIA INST OF TECH ATLANTA ENGINEERING EXPERIMENT --ETC F/G 17/9
ENVIRONMENT AND RADAR OPERATION SIMULATOR.(U)
MAR 76 S N COLE, A R CLAYTON, R C MICHELSON DAAB07-74-C-0272
UNCLASSIFIED ECOM-74-0272-6 NL

| OF |
AD
A034676

END

DATE
FILMED
2-77

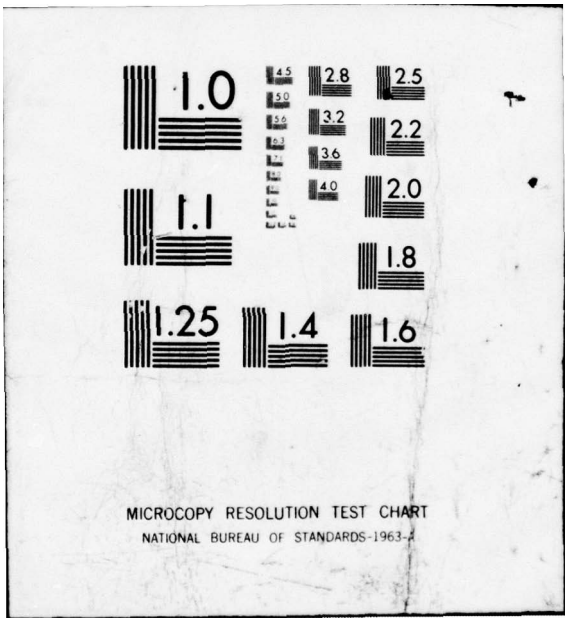
1.0
1.1
1.25
1.4
1.6
1.8
2.0
2.2
2.5
2.8
3.2
3.6
4.0
4.5
5.0
5.6
MICROCOPY RESOLUTION TEST CHART
NATIONAL BUREAU OF STANDARDS-1963-A

RESEARCH AND DEVELOPMENT TECHNICAL REPORT

REPORT ECOM-74-0272-6

ENVIRONMENT AND RADAR OPERATION SIMULATOR

By

S.N. Cole
A.R. Clayton
R.C. Michelson
E.S. Sjoberg

Engineering Experiment Station
Georgia Institute of Technology
Atlanta, Georgia 30332

March 1976

Sixth Quarterly Report for Period 1 October 1975 through 31 December 1975

Prepared for

ECOM

US ARMY ELECTRONICS COMMAND FORT MONMOUTH, NEW JERSEY 07703

NOTICES

Disclaimers

The findings in this report are not to be construed as an official Department of the Army position, unless so designated by other authorized documents.

The citation of trade names and names of manufacturers in this report is not to be construed as official Government indorsement or approval of commercial products or services referenced herein.

Disposition

Destroy this report when it is no longer needed. Do not return it to the originator.

UNCLASSIFIED

SECURITY CLASSIFICATION OF THIS PAGE (When Data Entered)

REPORT DOCUMENTATION PAGE

READ INSTRUCTIONS BEFORE COMPLETING FORM

1. REPORT NUMBER: ECOM-74-0272-6	2. GOVT ACCESSION NO.
3. RECIPIENT'S CATALOG NUMBER	
4. TITLE (and Subtitle): ENVIRONMENT AND RADAR OPERATION SIMULATOR.	5. TYPE OF REPORT & PERIOD COVERED: Sixth Quarterly rept. no. 6, 1 Oct 75 – 31 Dec 75
	6. PERFORMING ORG. REPORT NUMBER
7. AUTHOR(s): S. N. Cole, E. S. Sjoberg, A. R. Clayton, R. C. Michelson	8. CONTRACT OR GRANT NUMBER(s): DAAB07-74-C-0272
9. PERFORMING ORGANIZATION NAME AND ADDRESS: Georgia Institute of Technology, Atlanta, Georgia 30332	10. PROGRAM ELEMENT, PROJECT, TASK AREA & WORK UNIT NUMBERS: DA Proj C8-3-05107-05-C8-CA; AMC Proj 1S7-62703-D-H93-P1-06; AMC Code 672703-12-H93-P1-06
11. CONTROLLING OFFICE NAME AND ADDRESS: Commander, US Army Electronics Command, AMSEL-CT-R, Fort Monmouth, NJ 07703	12. REPORT DATE: March 1976
	13. NUMBER OF PAGES: 22
14. MONITORING AGENCY NAME & ADDRESS (if different from Controlling Office): 28 p.	15. SECURITY CLASS. (of this report): UNCLASSIFIED
	15a. DECLASSIFICATION/DOWNGRADING SCHEDULE

16. DISTRIBUTION STATEMENT (of this Report)

Approved for public release; distribution unlimited

1S762703D H93 P1

17. DISTRIBUTION STATEMENT (of the abstract entered in Block 20, if different from Report)

18. SUPPLEMENTARY NOTES

19. KEY WORDS (Continue on reverse side if necessary and identify by block number)

Signal Synthesis	Real-Time Simulation
Clutter Synthesis	Radar Simulation
Digital Filter Design	Radar Target Simulation
Pseudo-Random Numbers	Radar Clutter Simulation

20. ABSTRACT (Continue on reverse side if necessary and identify by block number)

This report summarizes activities during the sixth quarter of a program sponsored by the U.S. Army Electronics Command (ECOM), directed toward the design of an Environment and Radar Operation Simulator (EROS). The analysis of clutter-simulation digital filters has been directed toward determining the effect of filter parameters on the filter's output statistics. The feedback multipliers control the shape of the spectrum, and formulas are given relating the multiplier values to spectral characteristics. Parameters of the pseudo-

(CONTD.)

DD FORM 1 JAN 73 1473 EDITION OF 1 NOV 65 IS OBSOLETE

UNCLASSIFIED

SECURITY CLASSIFICATION OF THIS PAGE (When Data Entered)

153850

ABSTRACT (Contd.)

random number generator and other filter parameters control clutter amplitude distribution. An algorithm is provided for computing these parameters from given amplitude-distribution constraints. Digital hardware design has included the clutter filters, clutter azimuth weighting, the target processor, and several frequently used modules. Real-time software design has been directed toward the executive control program, which coordinates the computer's target, clutter, and display activities.

PREFACE

This report was prepared at the Georgia Tech Engineering Experiment Station under Contract No. DAAB07-74-C-0272. The work covered by this report was performed in the Applied Engineering Laboratory under the supervision of Dr. H. A. Ecker and Mr. J. L. Eaves, Director of the Applied Engineering Laboratory and Chief of the Radar Technology Division, respectively. The progress reported herein was performed during the sixth quarter of a program to develop an environment and radar operation simulator (EROS) to be used in testing radar receivers and components.

The contributions of Mr. E. R. Flynt of the Engineering Experiment Station staff and Dr. R. W. Schafer of the Georgia Tech School of Electrical Engineering are acknowledged. This project is being monitored by Mr. Reinhard G. Olesch and Mr. Otto E. Rittenbach of the U.S. Army Electronics Command, and their helpful suggestions are acknowledged.

TABLE OF CONTENTS

LIST OF FIGURES

1. INTRODUCTION

This report covers work performed during the period 1 October 1975 through 31 December 1975, the sixth quarter of the 30-month program to design and build an Environment and Radar Operation Simulator (EROS). Work has continued during the past quarter on the analysis of the clutter filters and on specifications for the real-time software. In addition, breadboarding and printed circuit layout have begun for portions of the EROS digital hardware. The analysis presented in Section 2 treats the dependence of clutter statistics on the digital filter parameters. The formulas derived in this section will be applied in the scenario preparation computer programs. Section 3 summarizes digital hardware implementation activities. In particular, the functions performed by the target processor and the clutter azimuth weighting hardware are described. The real-time executive control program coordinates the target, clutter, and display functions performed by PDP-11 computer during simulation. A summary of the specifications for this executive is provided in Section 4.

2. CLUTTER DIGITAL FILTER ANALYSIS

2.1 Introduction

Clutter return in EROS is simulated by applying digital noise (random numbers) to the digital filters whose parameters correspond to the statistics of the 544 simulated clutter cells. The requirements for the filters and the structure of the proposed hardware realization have been treated in Section 2 of the Third and Fifth EROS Quarterly Reports. During the past quarter, investigations have pursued questions of filter behavior and output statistics as functions of the filter parameters.

2.2 Dependence of Filter Behavior on Feedback Multipliers

The following is a reformulation and amplification of results reported in Section 2 of the Fifth EROS Quarterly Report. The (complex) digital filter which synthesizes the moving portion of clutter has two delay elements, whose outputs at time nT (after the nth iteration) are denoted by $w_1(nT)$ and $w_2(nT)$. The calculations performed by the filter are described by the equations

$$w_1((n+1)T) = \alpha_1 w_1(nT) + \alpha_2 w_2(nT) + x(nT) \qquad (1)$$

$$w_2((n+1)T) = w_1(nT)$$

$$y(nT) = \beta w_1(nT)$$

where

$x(nT)$ is the sequence of complex random inputs;

α_1, α_2, and β are (real) parameters that control the clutter statistics; and

$y(nT)$ is the sequence representing the sampled complex envelope of clutter return.

The filter will be implemented in the form of two identical modules; one will generate real components of $y(nT)$ for the 544 cells illuminated within an antenna beam, and the other will generate imaginary components.

The parameter β determines the radar cross section of the moving part of clutter and is discussed further in Section 2.3 of this report. The parameters α_1 and α_2 are the feedback multipliers that determine the spectral behavior of the clutter. For certain values of α_1 and α_2 there corresponds a two-pole analog filter from which α_1 and α_2 can be derived via the impulse-invariant method. If the poles of this analog filter are complex at

$$\omega_p e^{\pm j\theta}$$

$$\alpha_1 = 2e^{\omega_p T \cos\theta} \cos(\omega_p T \sin\theta), \text{ and} \tag{2}$$

$$\alpha_2 = -e^{2\omega_p T \cos\theta} .$$

These formulas were introduced with Equation (8) of the Fifth EROS Quarterly Report. The other possibility is that two poles may both be real at $\omega_p \pm D$. Then

$$\alpha_1 = 2e^{-\omega_p T} \cosh(DT) \tag{3}$$

$$\alpha_2 = -e^{-2\omega_p T} .$$

Clearly $\alpha_1^2 + 4\alpha_2$ is negative in the complex-roots case and positive in the real roots case. The quantity $\alpha_1^2 + 4\alpha_2$ serves as a discriminant for the digital filters. Expressions can be derived for the inverses of the transformations (2) and (3). If the discriminant is negative (complex-roots case), the analog poles are at

$$\omega_p e^{\pm j\theta} = \frac{1}{T}\left[-\frac{1}{2}\ln(-\alpha_2) \pm j\cos^{-1}\left(\frac{\alpha_1}{2\sqrt{-\alpha_2}}\right)\right] . \tag{4}$$

If the discriminant is positive, the analog poles are at

$$\omega_p \pm D = \frac{1}{T}\left[-\frac{1}{2}\ln(-\alpha_2) \pm \cosh^{-1}\left(\frac{\alpha_1}{2\sqrt{-\alpha_2}}\right)\right] . \tag{5}$$

The frequency response of the analog filter is denoted by $H_a(j\omega)$. The cutoff frequency ω_c has been defined[1] such that

$$\left| H_a(j\omega_c) \right|^2 = \frac{1}{2} \left| H_a(0) \right|^2 \quad .$$

Then for the complex-roots case ω_c is related to $\omega_p e^{\pm j\theta}$ according to the formulas

$$\omega_c = \omega_p \sqrt{-\cos 2\theta + \sqrt{1 + \cos^2(2\theta)}} \qquad (6)$$

$$\omega_p = \omega_c \sqrt{\cos 2\theta + \sqrt{1 + \cos^2(2\theta)}} \quad .$$

In the real-roots case ω_c is related to $\omega_p \pm D$ according to the formulas

$$\omega_c = \sqrt{-D^2 - \omega_p^2 + \sqrt{2D^4 + 2\omega_p^4}} \qquad (7)$$

$$\omega_p = \sqrt{D^2 + \omega_c^2 + \sqrt{2\omega_c^4 + 4\omega_c^2 D^2}}$$

The one-pole digital filter is realized by setting $\alpha_2 = 0$. In this case

$$\omega_p = \omega_c = -\frac{1}{T} \ln \alpha_1 \quad .$$

The one-pole digital filter is actually a special case of the two-pole filter where one of two real roots is at 0 in the z plane.

The dependence of the filter's spectral behavior upon α_1 and α_2 is illustrated in Figure 1. The portion of the (α_1, α_2) plane used in the EROS implementation hardware is the triangle bounded by the lines $\alpha_1 = 0$, $\alpha_2 = -1$, and $\alpha_1 + \alpha_2 = 1$. The lines $\alpha_2 = -1$ and $\alpha_1 + \alpha_2 = 1$ represent boundaries of two of the stability conditions. The third

---

[1] c.f. Section 2.2 of the Fifth EROS Quarterly Report.

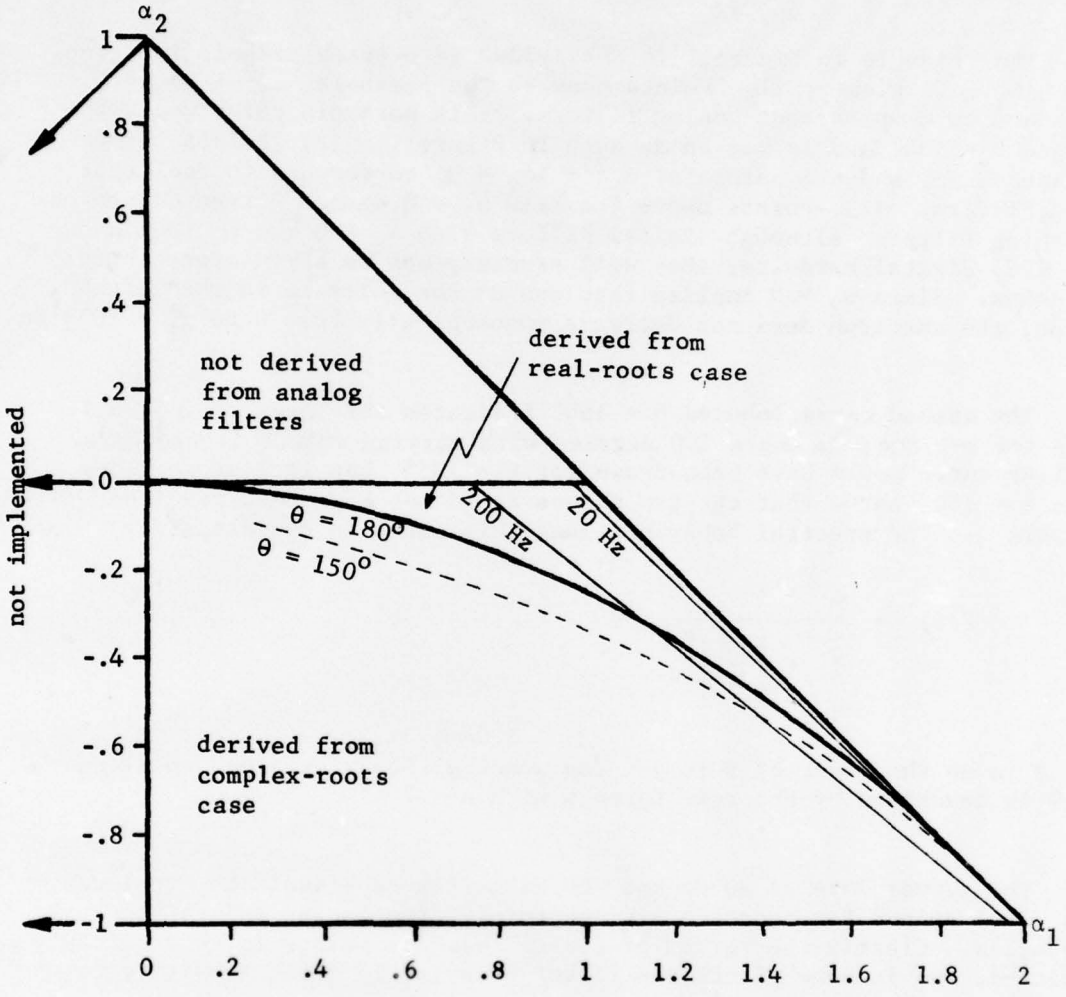

Figure 1. Dependence of Filter Behavior on (α_1, α_2).

stability-condition boundary, $\alpha_2 - \alpha_1 = 1$, does not come into play, because EROS implementation restricts α_1 to be positive. Negative values of α_1 would not be of interest in clutter simulation because the corresponding filters have band-pass behavior instead of the desired low-pass behavior.

The triangle in Figure 1 is subdivided into three principal regions of the (α_1, α_2) plane. (1) Points beneath the parabola, $\alpha_1^2 + 4\alpha_2 = 0$, correspond to complex-root analog filters. This parabola coincides with the case $\theta = 180°$ and is marked as such in Figure 1. (2) Points between the line $\alpha_2 = 0$ and the parabola, $\alpha_1^2 + 4\alpha_2 = 0$, correspond to real-root analog filters. (3) Points above the line $\alpha_2 = 0$ do not correspond to any analog filter. Although digital filters with $\alpha_2 > 0$ can be realized using EROS digital hardware, they will probably not be useful for clutter simulation. Since $\alpha_2 > 0$ implies that one of the poles is in the left-half z plane, the spectrum does not decrease monotonically from 0 to $\frac{1}{2T}$ = 2033 Hertz.

The dashed curve labeled $\theta = 150°$ indicates the locus of (α_1, α_2) points for s-plane pole angle 150 degrees with varying cutoff frequencies. A similar curve could have been drawn for $\theta = 135°$, but it lies so close to the $\theta = 150°$ curve that the two curves could not have been resolved in Figure 1. The spectral behavior along this curve is approximately

$$P(f) = \frac{1}{1 + \left| \frac{f}{f_c} \right|^n} ,$$

where n is on the order of 3 to 4. The spectral behavior along the line $\alpha_2 = 0$ is described by the same formula with n = 2.

The curves labeled 20 Hz and 200 Hz in Figure 1 indicate the locus of (α_1, α_2) points for constant s-plane cutoff frequencies and varying pole angles. Clearly the region of useful (α_1, α_2) points is very narrowly restricted, and in some places the filter behavior is quite sensitive to small changes in α_1 and α_2.

2.3 Statistics of Synthetic Clutter

The statistics describing the outputs from the EROS clutter filters were discussed in Section 5 of the Second EROS Quarterly Report and in Section 2 of the Third EROS Quarterly Report. The conclusions reached in these reports were dependent upon assumptions of ideal behavior by the random inputs; i.e. (1) zero mean and (2) uncorrelated samples. The EROS pseudo-random number generator described below approximates this behavior with very small deviations. Moreoever, the truncation errors

introduced by the α_1 and α_2 multipliers contribute additional noise inputs whose statistics also fail to satisfy these assumptions. Therefore, it is appropriate to examine the effect of such deviations upon the output statistics--the mean, variance, and power spectral density. In this development all random processes are assumed to be stationary and the following notation will be used. If u(nT) and v(nT) are random processes, and if X is a random variable, then

$E\{X\}$ = expected value of X

X^* = complex conjugate of X

μ_u = mean of u(nT) = $E\{u(nT)\}$

σ_u^2 = variance of u(nT) = $E\{|u(nT) - \mu_u|^2\}$

$R_u(mT)$ = autocorrelation of u(nT) = $E\{u(nT)\ u^*(nT + mT)\}$.

The cross covariance of u(nT) with v(nT) is defined as $E\{(u(nT) - \mu_u)(v^*(nT + mT) - \mu_v^*)\}$. The autocovariance of u is defined as the cross covariance u(nT) with u(nT) and it equals $R_u(nT) - |\mu_u|^2$.

The pseudo-random number generator[1] to be used in the EROS implementation model is described by Figure 2. It consists of 31 1-bit delay elements, an exclusive-or-gate, and decode logic to produce the two possible outputs $+\gamma$ or $-\gamma$. Let $\rho(nT_1)$ denote the sequence of outputs from this shift register. If the initial states of the 31 delay elements are not all zero, then $\rho(nT_1)$ has a cycle length of $p = 2^{31} - 1$. Of these p outputs $(p + 1)/2$ of them are $+\gamma$'s, and $(p - 1)/2$ of them are $-\gamma$'s. The relevant statistics of $\rho(nT_1)$ are

$$\mu_\rho = \gamma\, p^{-1} = \gamma(2^{31} - 1)^{-1}$$

$$\sigma_\rho^2 = \gamma^2 - \gamma^2\, p^{-2} = \gamma^2 - \mu_\rho^2 \qquad (8)$$

$$R_\rho(mT_1) = \begin{cases} \gamma^2 & m = np \\ \gamma^2 p^{-1} = -\gamma\,\mu_\rho & \text{otherwise} \end{cases}$$

---

[1] This design of the pseudo-random number generator and the statistics of the pseudo-random sequences are based on the book by Golomb, Solomon, W., Shift Register Sequences, Holden-Day Inc., Cambridge, Mass., 1967.

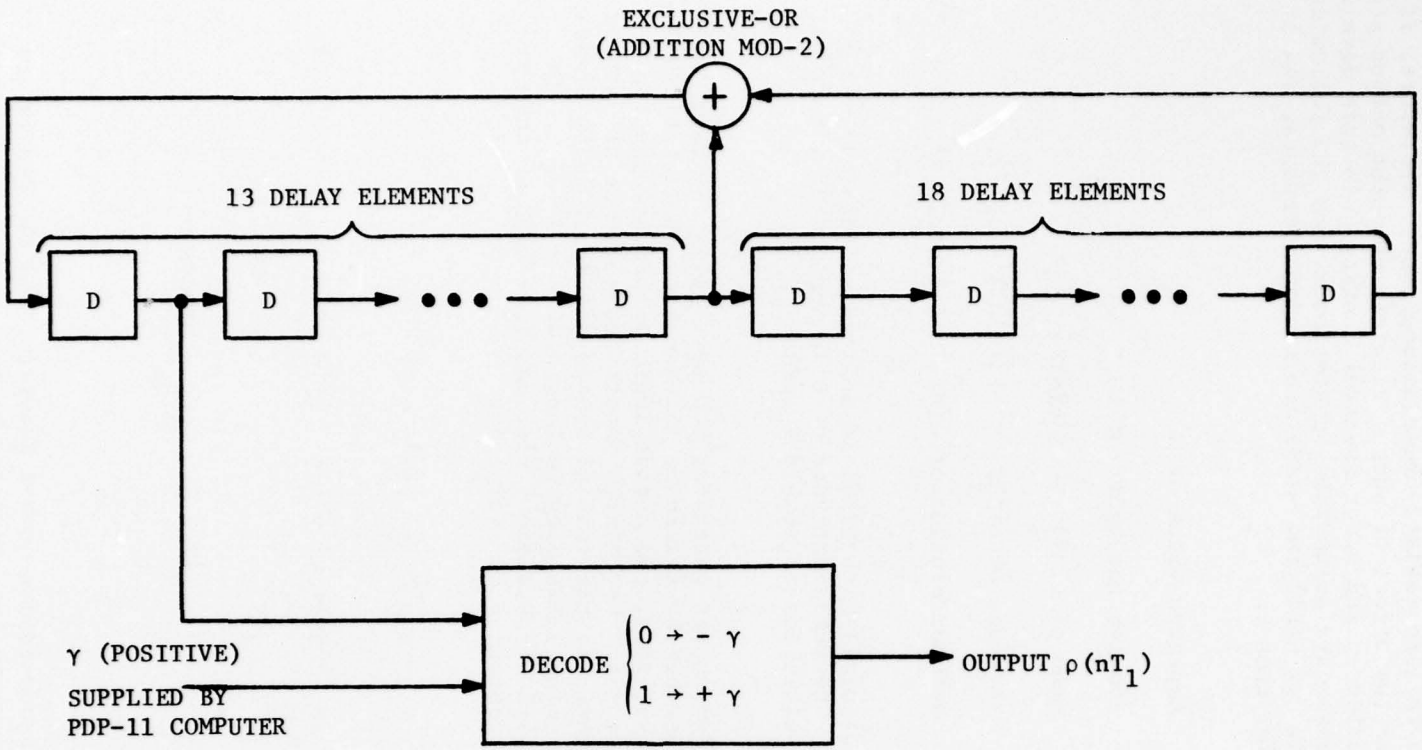

Figure 2. Pseudo-Random Number Generator.

Two pseudo-random inputs are required for each of the 544 filters during every Doppler cycle. Thus pseudo-random inputs are consumed at the rate of 1088 per Doppler cycle. Although the pseudo-random sequence is periodic, the period is exceedingly long. A portion of the pseudo-random sequence used on one of the 544 filters would not be reused on any of the other filters until 7.9 minutes later, and it would not be reused on the same filter until 2029 minutes later. Therefore, it is appropriate to treat the pseudo-random input sequence as aperiodic and to simplify the expression of R_ρ:

$$R_\rho(mT_1) = \begin{cases} \gamma^2 & m = 0 \\ -\gamma\ \mu_\rho & \text{otherwise} \end{cases} .$$

Let r(nT) denote the complex random input

$$r(nT) = \rho(mT_1) + j\ \ \rho(mT_1 + T_1) .$$

The statistics of r(nT) are readily derived:

$$\begin{aligned} \mu_r &= (1 + j)\ \mu_\rho \\ \sigma_r^2 &= 2(\gamma^2 - \mu_\rho^2) \end{aligned} \qquad (9)$$

$$R_r(mT) = \begin{cases} 2\gamma^2 & m = 0 \\ -2\gamma\mu_\rho & \text{otherwise} \end{cases}$$

The arithmetic performed by the digital filters assumes 16-bit 2's complement binary fractions; the binary point is assumed to be between the sign bit and the 15 fraction bits. During each computation cycle the products $(\alpha_1 - 1)\ w_1$ and $\alpha_2\ w_2$ are formed, and the 30 fraction bits of each (real and imaginary) component of the product is truncated to 15 bits; the low-order 15 bits are discarded. If [a] denotes the largest integer that does not exceed a, and if [a + jb] denotes [a] + j[b], then truncated products are expressed by $[2^{15}(\alpha_1 - 1)\ w_1]\ 2^{-15}$ and $[2^{15}\ \alpha_2\ w_2]\ 2^{-15}$.

Therefore the truncation errors are

$$e_1 = [2^{15} (\alpha_1 - 1) w_1] 2^{-15} - (\alpha_1 - 1) w_1$$

and (10)

$$e_2 = [2^{15} \alpha_2 w_2] 2^{-15} - \alpha_2 w_2 \quad .$$

The effects of truncation errors can be determined by treating e_1 and e_2 as additional random-number sources, since Equation (1) remains valid if

$$x(nT) = r(nT) + e_1 (nT) + e_2 (nT) \quad . \tag{11}$$

An exact statistical analysis of x(nT) is difficult, because the distributions of e_1 and e_2 depend upon the distribution of w_1. Although some analysis has already been performed to determine the distributions of e_1 and e_2, the investigations are continuing, and the results will be documented in a subsequent report. For the present discussion the following approximations are assumed.

(1) The cross covariance sequences of r with e_1, r with e_2, and e_1 with e_2 are identically 0.

(2) The autocovariance sequences of e_1 and e_2 are 0 for non-0 arguments.

From these assumptions and Equations (9) and (11) it follows that

$$\mu_x = \mu_r + \mu_{e_1} + \mu_{e_2} = (1 + j) \mu_\rho + \mu_{e_1} + \mu_{e_2}$$

$$\sigma_x^2 = \sigma_r^2 + \sigma_{e_1}^2 + \sigma_{e_2}^2 = 2(\gamma^2 - \mu_\rho^2) + \sigma_{e_1}^2 + \sigma_{e_2}^2$$

$$R_x(mT) = \begin{cases} 2(\gamma^2 - \mu_\rho^2) + \sigma_{e_1}^2 + \sigma_{e_2}^2 + |\mu_x|^2 & m = 0 \\ -2\gamma \mu_\rho - 2 \mu_\rho^2 + |\mu_x|^2 & \text{otherwise} \end{cases} \tag{12}$$

The unit-impulse response at output node w_1 (nT) is denoted by h(0), h(T), . . ., h(nT), ... Note that h(nT) is real. By the convolution formula the response w_1(nT) to the random input sequence x(nT) is

$$w_1 (nT) = \sum_{i=0}^{\infty} h(iT)\, x(nT - iT)$$

and

$$y(nT) = \beta \sum_{i=0}^{\infty} h(iT)\, x(nT - iT) \quad .$$

Therefore

$$\mu_y = \beta F \mu_x \quad , \tag{13}$$

where

$$F = \sum_{i=0}^{\infty} h(nT) \quad .$$

Moreover, from the convolution formula and the definition of the auto-correlation sequence

$$R_y(mT) = \beta^2 \sum_{i=0}^{\infty} \sum_{k=0}^{\infty} h(iT)\, h(kT)\, R_x (mT + iT - kT) \quad . \tag{14}$$

With the substitution of (12) into (14)

$$R_y(mT) = \beta^2 F^2 R_x(\text{non-0}) + \beta^2 [R_x(0) - R_x(\text{non-0})] \sum_{k=0}^{\infty} h(kT)\, h(kT - mT) \tag{15}$$

The variance σ_y^2 is derived immediately by evaluating $R_y(0) - |\mu_y|^2$

$$\sigma_y^2 = \beta^2 F^2 (- 2\gamma\mu_\rho - 2\mu_\rho^2) + \beta^2 G^2 (2\gamma^2 + \sigma_{e_1}^2 + \sigma_{e_2}^2 + 2\gamma\mu_\rho) \tag{16}$$

where G^2 is the sum of squares of the unit-impulse response

$$G^2 = \sum_{k=0}^{\infty} h^2 (kT) \quad .$$

The computations of F and G^2 are simplified by the following formulas,

$$F = \frac{1}{1 - \alpha_1 - \alpha_2}$$

$$G^2 = \frac{(1 - \alpha_2)}{(1 + \alpha_2)[(1 - \alpha_2)^2 - \alpha_1^2]} \quad . \tag{17}$$

The dependence of the clutter simulation upon radar cross section is taken into account by employing Equations (13) and (16). The procedure is as follows.

(1) Choose the quantity γ so that the magnitudes of w_1 and w_2 are significant but safely below overflow levels. For EROS implementation γ will be the largest power of 2 such that

$$\gamma \sum_{i=0}^{\infty} |h(iT)| < 1 \quad . \tag{18}$$

(2) All of the quantities in (16) except β can be determined independently. F and G^2 are computed with the aid of (17). The quantity μ_ρ equals $(2^{31} - 1)^{-1}$. The quantites μ_x, $\sigma_{e_1}^2$, and $\sigma_{e_2}^2$ can be calculated from a statistical analysis of e_1 and e_2. The quantity σ_y^2 can be determined from the specified radar cross section of the moving part of clutter. Therefore, β can be calculated by solving (15).

(3) Since the amplitude distribution of the simulated clutter is to be Ricean,[1] a complex constant K is added to y(nT) to force the resulting sum to have complex mean S. The quantity $|S|^2$ is proportional to the radar cross section of the immobile part of clutter, and the phase of S is randomly chosen during scenario preparation. Then from Equation (13)

$$S = K + \beta F \mu_x \, , \tag{19}$$

from which K can be determined with the aid of (17).

---

[1] Refer to Section 2.5 of the Third EROS Quarterly Report.

The power spectral density of the simulated clutter is the Fourier transform of $R_y(mT) + K\mu_y^* + K^*\mu_y + |K|^2$. Inspection of (15) indicates that this autocorrelation sequence assumes the form of a constant term plus an aperiodic term. The spectral specifications for the simulated clutter apply only to the aperiodic term, and the Fourier transform of this aperiodic term is easily determined by evaluating its z-transform at $z = e^{j\omega T}$. The result is proportional to $|H(e^{j\omega T})|^2$, where H(z) is the z-transform of h(nT). Therefore the spectral behavior is not adversely affected by the non-zero correlations between the samples from the pseudo-random number generator.

2.4 Next Quarter Plans

Filter analyses will continue next quarter supported by computer simulations. The investigation of truncation-error statistics will be pursued, with the intent of deriving algorithms for estimating their means and variances. Effort will also be directed toward deriving formulas which relate output variances to desired radar cross sections and to calibration conditions.

3. DIGITAL HARDWARE IMPLEMENTATION

3.1 Introduction

Digital hardware efforts during the past quarter have concentrated on the design of the clutter processor, on the design of the target processor, and on identifying frequently occurring functions that might be conducive to standardization as modules. In addition, two of the EROS digital hardware subsystems have been breadboarded and verified in concept and operation. Printed circuits (PC) layouts for the breadboarded subsystems are presently under construction.

3.2 Clutter Processor

The clutter hardware has been divided into seven major units which include the digital filter, pseudo-random number generator, azimuth weight generator, azimuth starting address generator, timing and control unit, cell counter, and computer data interface. Detailed block diagrams and timing charts have been formulated for each major component except the timing and control unit.

3.3 Clutter Azimuth Weighting

The azimuth position of the AN/PPS-15 radar is supplied to EROS as a 10-bit word with a resolution of one 1024th of a circle. With 256 clutter columns per circle,[1] there are four azimuth positions in each clutter column. A new azimuth reading is made each antenna cycle, which is defined as 256 Doppler cycles[2] (i.e., 256 x 240 μsec). At a constant scan rate of 90 mil/second, the 10-bit azimuth position word will change by slightly less than one least significant bit during the antenna cycle.

As shown in the Fourth EROS Quarterly Report, there will be 17 clutter columns and 32 range rings for a total of 544 clutter cells, simulated at any instant in time. One sample from each clutter cell will be generated during each Doppler cycle. The azimuth weight is the same for all cells within a column, and is calculated using the formula

---

[1] c.f. Fourth EROS Quarterly Report Section 2.3.

[2] c.f. Fourth EROS Quarterly Report Section 2.3.

$$w(\theta_i) = \sqrt{\frac{1}{\Delta\theta} \int_{\theta_i - \frac{\Delta\theta}{2}}^{\theta_i + \frac{\Delta\theta}{2}} g^2(\phi)\, d\phi} \qquad (20)$$

where

$g(\phi)$ = one way power antenna pattern normalized to one at the peak;

$\Delta\theta$ = clutter column width = 25 mils;

θ_i = azimuth position of a clutter column relative to the antenna beam position

Notice that even though $g(\phi)$ extends over only 16 clutter columns, the smearing effect of integrating over a clutter column width ($\Delta\theta$) for each value of θ_i, causes the weights, $w(\theta_i)$, to have non-zero values over 17 clutter columns. Since there are four possible azimuth readings per column there are 68 possible azimuth weights. These 68 weights are stored in a random access memory during simulation initialization.

As noted in the appendix of the Fifth EROS Quarterly Report, it is necessary to interpolate between successive antenna azimuth readings to reduce spurious signals to an acceptable level. This requirement is met for the clutter azimuth weighting by interpolating both the angle and weight in one operation. For each of two successive azimuth readings, the corresponding arrays of 17 weights,

$$w_1, w_2, \ldots, w_{17}$$

and

$$w_1', w_2', \ldots, w_{17}'$$

are read from memory. An array weight increment

$$\Delta w_1, \Delta w_2, \ldots, \Delta w_{17}$$

is then computed such that

$$w_i = \frac{w_i' - w_i}{256} \quad .$$

The interpolated weights for the 17 clutter columns can thus be computed recursively for each Doppler cycle according to the formula

$$\left.\begin{aligned} w_i(0) &= w_i \\ w_i(k+1) &= w_i(k) + \Delta w_i \end{aligned}\right\} \qquad \begin{aligned} i &= 1, \ldots, 17 \\ k &= 0, \ldots, 254 \end{aligned}$$

3.4 Target Processor

The purpose of the target processor is to combine in-phase and quadrature target samples, range-ring numbers, and antenna weights to produce a composite target signal. Each target sample is multiplied by the appropriate weight and stored in the double-buffered random access memory (RAM) of Figure 3. Since the computer and the subsequent EROS digital hardware are asynchronous, the RAM provides the necessary interface. Target samples with identical range-ring numbers are added together and then added to the composite clutter sample with the same range-ring number. Throughout this process, synchronization with the clutter processor is maintained by an interchange of status flags.

3.5 Standard Modules

In Figure 3, a block diagram of the target processor, note that there is a repetition of certain functions (e.g., data selectors, 1k by 16-bit memory arrays, 20-bit integrators). These, and four other functions have been chosen for implementation as standard modules. This design methodology will take advantage of the fact that PC boards can be reproduced any number of times. Once a standard module on a PC board has been debugged, the module can serve as a building block for higher assemblies, the designer having only to understand the input-output characteristics of the module.

The seven most frequently occurring functions appearing in the EROS digital processor are

- 16 by 16-bit multiplier
- 1k by 16-bit memory array
- 20-bit adder
- 20-bit integrator

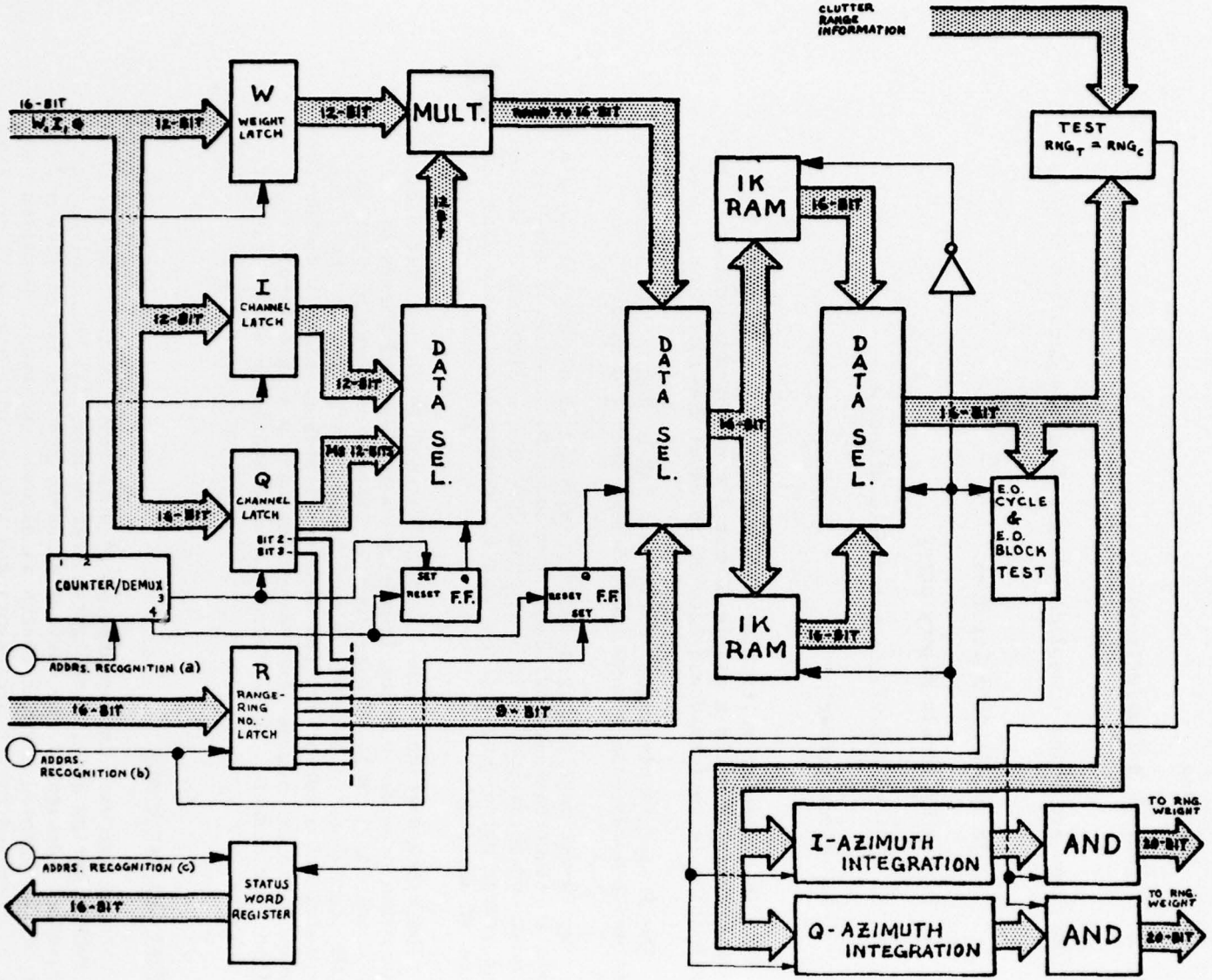

Figure 3. Block Diagram of EROS Target Processor.

- 20-bit data selector
- clocking
- output buffer/drivers.

These functions are being consolidated into four standardized modules.

1. 16 by 16-bit multiplier
2. 1k by 16-bit memory array
3. 20-bit adder/integrator/data selector
4. clock/buffer

The 16 by 16-bit multiplier module multiplies two 16-bit 2's complement words to yield a single 32-bit 2's complement product. This multiplication is performed and latched in under 200 nsec worst case.

The 1k and 16-bit memory array is a RAM having a word length of 16 bits and a worst-case access time of less than 100 nsec.

The 20-bit adder/integrator/data selector is a versatile module that can be electronically switched from adder to integrator and back. Worst case adder throughput is less than 200 nsec. Simple modification (adding jumper wires) enables the unit to perform purely as a data selector if desired.

The clock portion of the clock/buffer module is actually a divider circuit which provides various frequency multiples and phases of the system clock ($\simeq$ 10 MHz). These clocking signals are used by virtually all EROS components to maintain synchronism. The buffer of the clock/buffer module is a set of drivers used to distribute signals coming into a drawer of circuit boards thus presenting only a single input load per signal per drawer. The drivers are also available as interdrawer cable drivers.

3.6 Next Quarter Goals

Actual hardware implementation of such units as the computer interface, PROM blasting unit, and digital test system will be complete early next quarter. Design of the various standard modules is complete and layout of the printed circuit boards is already underway. Detailed design of the clutter and target processors and related circuitry will continue at present level.

4. SOFTWARE

4.1 Real-Time EROS Executive Routine

A detailed flow chart description of the real-time EROS executive routine for Target Modes[1] 1 and 2 has been developed during the past quarter. This routine is based on target data scheduling as described in the Fifth EROS Quarterly Report.

The executive routine will control the simulated status of the targets and clutter as functions of time and the antenna azimuth. It will invoke the target and clutter processing routines at scheduled intervals and invoke the display routine as time permits.

A new antenna azimuth value will be read from hardware after each 256 Doppler cycles, i.e., at a frequency of 16.28 times per second. One complete loop of the executive routine will be executed at this same frequency. The clock that synchronizes executions of the executive routine is a flag set by the EROS digital hardware each time the target processor accesses a new buffer of target data. In Target Modes 1 and 2 this will occur at a frequency of 32.56 times per second or twice the antenna read frequency. Thus, a new execution of the executive loop will begin at every other flag setting.

A simplified flow chart of the executive routine is shown in Figure 4.

4.2 Core Tables and Data Buffers

A number of tables and data buffers will be maintained in core by the real-time software. One table will contain information needed for scheduling target data. A second table will provide sampled antenna pattern weights. Buffers for target and clutter data will be used for disk input.

These tables and buffers have been defined and documented in sufficient detail to permit an estimate of their core requirements.

---

[1] See EROS Fifth Quarterly Report for definitions of target modes.

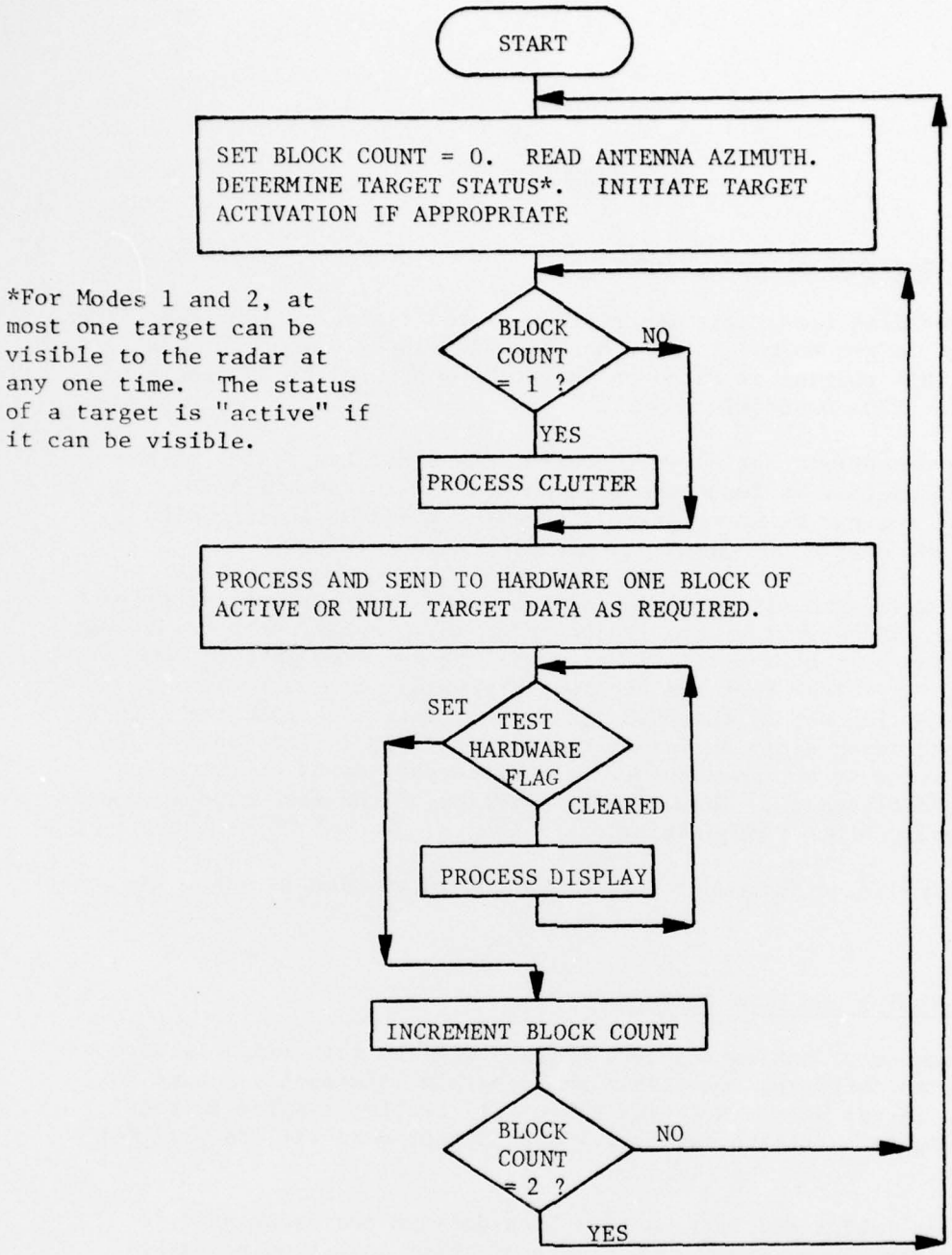

Figure 4. Flow Chart of EROS Real-Time Executive Routine.

Target Scheduling Table	600 words
Antenna Pattern Table	4096 words
Target Data Input Buffer	6144 words
Clutter Data Input Buffer	3726 words
Total	14,566 words

If core space becomes critical, certain reductions can be made at the expense of increased processing time.

4.3 Next Quarter Plans

During next quarter, the executive routine for Target Modes 1 and 2 will be coded and debugged. Design of the target routine for Mode 2 will be continued. Work will continue on drafting a plan for EROS software development, identifying all programs and scheduling their development.

5. SUMMARY OF NEXT QUARTER PLANS

The design and implementation of the EROS feasibility model will continue during the next quarter. Analysis efforts will support the development of specifications for scenario preparation software; in particular the investigations will concentrate on the statistics of truncation errors and on the scaling for radar cross section. Digital hardware implementation of the computer interface, the PROM blasting unit, and the digital test system should be completed during the next quarter. Detailed design of the target and clutter processors will be pursued. Plans for real-time software development include completion of the real-time executive control program for Modes 1 and 2.

HEADQUARTERS
US ARMY ELECTRONICS COMMAND
FORT MONMOUTH, NJ 07703

AMSEL-CT-R

TITLE OF REPORT: Environment and Radar Operation Simulator (EROS)
CONTRACT NUMBER: DAAB-74-C-0272
CONTRACTOR: Georgia Institute of Technology

DISTRIBUTION LIST

	NR. OF COPIES
Defense Documentation Center ATTN: DDC-TCA Cameron Station (Bldg 5) Alexandria, VA 22314	1
Defense Intelligence Agency ATTN: DIADT-3C Washington, DC 20301	1
Dir, National Security Agency ATTN: TDL Ft George G. Meade, MD 20755	1
Dir, Defense Nuclear Agency ATTN: Technical Library Washington, DC 20305	1
Naval Ship Engineering Center ATTN: Code 6179B Prince Georges Center Bldg Hyattsville, MD 20782	1
Cdr, Naval Electronics Lab Center ATTN: Library San Diego, CA 92152	1
Cdr, US Naval Ordnance Lab ATTN: Technical Library White Oak, Silver Spring, MD 20910	1
Commandant, Marine Corps HQ US Marine Corps ATTN: Code A04C Washington, DC 20380	1

AMSEL-CT-R
Distribution List for Contract DAAB07-74-C-0272, Georgia Inst of Technology

	NR. OF COPIES
Communications-Electronics Division Development Center Marine Corps Dev & Educ Command Quantico, VA 22134	1
Cdr, US Naval Weapons Lab ATTN: KEB-2F(FENN) Dahlgren, VA 22448	1
Rome Air Development Center ATTN: Documents Library (TDLD) Griffiss AFB, NY 13440	1
HQ ESD (TRI) L. G. Hanscom Field Bedford, MA 01730	1
Air Force Avionics Laboratory ATTN: AFAL/DOT (STINFO) Wright-Patterson AFB, OH 45433	1
Armament Development & Test Center ATTN: SSLT Eglin AFB, FL 32542	1
HQ, Air Force Systems Command ATTN: DLTE Andrews AFB Washington, DC 20331	1
Air Force Weapons Laboratory ATTN: Technical Library (SUL) Kirtland AFB, NM 87117	1
Cdr, US Army Training & Doctrine Cmd ATTN: ATTS-X Fort Monroe, VA 23651	1
HQDA (DAFD-CN) Washington, DC 20310	1
HQDA (DACE-ED) Washington, DC 20314	1

AMSEL-CT-R

Distribution List for Contract DAAB07-74-C-0272, Georgia Inst of Technology

	NR. OF COPIES
Ofc, Asst Secy of the Army (R&D) ATTN: Assistant for Research Rm 3-E-379, The Pentagon Washington, DC 20310	1
Cdr, US Army Training & Doctrine Cmd ATTN: ATCD-SI Fort Monroe, VA 23651	1
HQDA (DARD-ARP/Dr. R. B. Watson) Washington, DC 20310	1
Cdr, US Army Materiel Command ATTN: AMCRD-O 5001 Eisenhower Ave Alexandria, VA 22333	1
Cdr, US Army R&D Group (Far East) APO, San Francisco, CA 96343	1
Cdr, USA Missile Command Redstone Scientific Info Center ATTN: Ch, Document Section Redstone Arsenal, AL 35809	1
Cdr, US Army Training & Doctrine Cmd ATTN: ATCE Fort Monroe, VA 23651	1
Cdr, USA Weapons Command ATTN: AMSWE-REF Rock Island, IL 61201	1
Cdr, US Army Combined Arms Combat Dev Activity ATTN: ATCAIC Fort Leavenworth, KS 66027	1
HQ, USA Aviation Systems Command ATTN: AMSAV-C-AD P. O. Box 209 St. Louis, MO 63166	1

AMSEL-CT-R
Distribution List for Contract DAAB07-74-C-0272, Georgia Inst of Technology

	NR. OF COPIES
Cdr, Harry Diamond Laboratories ATTN: Library Washington, DC 20438	1
Cdr, USA Foreign Sci & Tech Cen ATTN: AMXST-IS1 220 Seventh St., NE Charlottesville, VA 22901	1
Cdr, USA Picatinny Arsenal ATTN: SMUPA-VC5 (Mr. P. Kisatsky) Bldg 350 Dover, NJ 07801	1
Cdr, Frankford Arsenal ATTN: Library, H1300, Bldg 51-2 Philadelphia, PA 19137	1
Crd, White Sands Missile Range ATTN: STEWS-RE-10 (Mr. G. Galos) White Sands Missile Range, NM 88002	1
Dir, USA Ballistic Research Lab ATTN: AMXBR-VL (Mr. D. L. Riggotti) Aberdeen Proving Ground, MD 21005	1
Cdr, USA Mat & Mech Rsch Center ATTN: AMXMR-ATL (Tech Library Br) Watertown, MA 02172	1
President, USA Artillery Board Fort Sill, OK 73503	1
Cdr, Aberdeen Proving Ground ATTN: Technical Library, Bldg 313 Aberdeen Proving Ground, MD 21005	1
Cdr, USA Electronic Proving Ground ATTN: STEEP-MT Fort Huachuca, AZ 85613	1
Cdr, USASA Test & Evaluation Center Fort Huachuca, AZ 85613	1

AMSEL-CT-R
Distribution List for Contract DAAB07-74-C-0272, Georgia Inst of Technology

	NR. OF COPIES
USA Research Office - Durham ATTN: Dr. Robert J. Lontz Box CM, Duke Station Durham, NC 27706	1
Cdr, USA Mobility Eqpt R&D Center ATTN: Tech Docu Cntr, Bldg 315 Fort Belvoir, VA 22060	
USA Security Agency ATTN: IARD Arlington Hall Sta, Bldg 420 Arlington, VA 22212	1
Cdr, USA Tank-Automotive Command ATTN: AMSTA-RH-FL Warren, MI 48090	1
Technical Support Directorate ATTN: Technical Library, Bldg 3330 Edgewood Arsenal, MD 21010	1
Cdr, US Army Combined Arms Combat Dev Activity ATTN: ATCACC Fort Leavenworth, KS 66027	1
Cdr, USA Dugway Proving Ground Library ATTN: STEDP-TL (Tech Library) Dugway, UT 84022	1
Cdr, Yuma Proving Ground ATTN: STEYP-AD (Tech Library) Yuma, AZ 85364	1
Cdr, US Army Materiel Command ATTN: AMCRD-R 5001 Eisenhower Avenue Alexandria, VA 22333	1
Commandant, US Army Infantry Sch ATTN: ATSIN-CTD Fort Benning, GA 31905	1

AMSEL-CT-R
Distribution List for Contract DAAB07-74-C-0272, Georgia Inst of Technology

	NR. OF COPIES
Commandant, USA Field Artillery School ATTN: Target Acquisition Dept Fort Sill, OK 73503	1
Cdr, USA Systems Analysis Agency ATTN: AMSRD-AMB (Mr. A. Reid) Aberdeen Proving Ground, MD 21005	1
Cdr, USA Tank-Automotive Cmd ATTN: AMSTA-Z (Dr. J. Parks) Warren, MI 48090	1
Ch, Missile EW Technical Area EW Laboratory (ECOM) White Sands Missile Range, NM 88002	1
Ch, Intelligence Mat Dev Ofc EW Laboratory (ECOM) Fort Holabird, MD 21219	1
NASA Sci & Tech Info Facility ATTN: Acquisitions Br (S-AK/DL) P. O. Box 33 College Park, MD 20740	1
Target Signature Analysis Center Willow Run Labs - Inst of Science & Technology University of Michigan P. O. Box 618 Ann Arbor, MI 48107	1
Remote Area Conflict Info Center Battelle Memorial Institute 505 King Avenue Columbus, OH 43201	1
Martin Marietta Corporation ATTN: MS 0452 (Lynes) P. O. Box 179 Denver, CO 80201	1
Cdr, Rome Air Development Center ATTN: Mr. John C. Cleary/OCSA Griffiss AFB, NY 13441	1

AMSEL-CT-R

Distribution List for Contract DAAB07-74-C-0272, Georgia Inst of Technology

NR. OF COPIES

Cdr, US Army Electronics Command
Fort Monmouth, NJ 07703

1	AMSEL-NV-D	1	AMSEL-VL-D	1	AMSEL-MA-MP	1	AMSEL-PA
1	AMSEL-WL-D	1	AMSEL-CT-R	1	AMSEL-MS-TI	1	AMSEL-RD
1	AMSEL-NL-D	1	AMSEL-SI-CB	1	AMSEL-GG-RD	1	TDC-LNO

This contract is supervised by Radar Technical Area, Combat Surveillance and Target Acquisition Laboratory, US Army Electronics Command, Fort Monmouth, New Jersey 07703. Tel: Eatontown, NJ, Area Code (201) 596-1407.